NUMERICAL SIMULATION AND PARAMETER ANALYSIS OF LIQUID NITROGEN COOLING FOR HIGH TEMPERATURE GRANITES

by

Chun-Bo ZHOU[a], Shan-Jie SU[b*], Cheng-Zheng CAI[c], and Feng GAO[c]

[a] School of Science, Qingdao University of Technology, Qingdao, China
[b] School of Civil Engineering, Xuzhou University of Technology, Xuzhou, China
[c] State Key Laboratory of Intelligent Construction and Healthy Operation and Maintenance of Deep Underground Engineering, China University of Mining and Technology, Xuzhou, China

Original scientific paper
https://doi.org/10.2298/TSCI2502463Z

Liquid nitrogen stimulation has important application value in the fields of deep geothermal development, and unconventional oil and gas reservoir exploitation. It is difficult to experimentally observe the evolution of temperature and cryogenic-induced stress inside the rock during the cooling process. Numerical simulation complements the experimental difficulties. In this study, the liquid nitrogen cooling process of high temperature granite under different parameters is studied by numerical simulation. The results show that a higher heat transfer coefficient and model initial temperature enhance the heat transfer efficiency of the cooling process, thus resulting in more severe cryogenic-induced stresses. Young's modulus and expansion coefficient are independent of the temperature distribution during the cooling process. Higher Young's modulus amplifies stress under identical thermal contraction constraints. Higher expansion coefficients enhance the thermal strains and thermal strain incompatibility, thus elevating the cryogenic-induced stresses. This study will provide the theoretical basis for the application of liquid nitrogen in reservoir stimulation.

Key words: *liquid nitrogen, heat transfer coefficient, initial temperature, Young's modulus, expansion coefficient*

Introduction

Liquid nitrogen stimulation, as an effective means of inducing thermal damage in rocks, has important application value in the fields of deep geothermal development, and unconventional oil and gas reservoir exploitation [1]. For deep geothermal reservoirs, by applying liquid nitrogen (−196 °C) in contact with high temperature rock (above 150 °C), the technique triggers a drastic unsteady temperature gradient inside the rock, which induces thermal stresses and damage inside the rock [2].

Experimental tools provide key support for revealing the rock damage induced by liquid nitrogen cooling. Advanced instrumentation, including acoustic emission [3], nuclear magnetic resonance [4], and micro-computed tomography scanning [5], has enabled quantitative assessment of liquid nitrogen-induced damage progression. Experimental data systematically demonstrate that a single liquid nitrogen cooling reduces the uniaxial compressive strength [6], P-wave velocity [6], and increases permeability [7], depending on initial rock temperature and

* Corresponding author, e-mail: sushanjie@xzit.edu.cn

rock types [7]. In addition, fracture modes are also altered by liquid nitrogen cooling [8]. These are attributed to the generation of cryogenic-induced stresses during the cooling process [9]. The cooling rate is usually related to the heat transfer coefficient and rock initial temperature [10], which in turn affects the generation of cryogenic-induced stresses. Cryogenic-induced stresses are also related to the rock's physical properties (*e.g.* Young's modulus and coefficient of expansion) [11]. The liquid nitrogen cooling process has not been adequately studied. It is difficult to experimentally observe the evolution of temperature and cryogenic-induced stress inside the rock during the cooling process. Numerical simulation complements the experimental difficulties. The thermal-mechanical coupling finite element model can accurately calculate the rock temperature and stress during liquid nitrogen cooling by solving the transient heat conduction equation and the thermoelasticity equation [9, 11].

In this study, the liquid nitrogen cooling process of high temperature granite is studied by numerical simulation. The effects of heat transfer coefficient, rock initial temperature, Young's modulus, and expansion coefficient on the temperature and cryogenic-induced stress of granite are investigated. This study will provide the theoretical basis for the application of liquid nitrogen in reservoir stimulation.

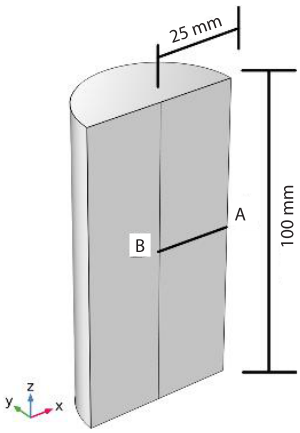

Figure 1. Model description

Model description

The standard specimen subjected to the liquid nitrogen cooling is simplified to a 2-D axisymmetric model with a length of 100 mm and a radius of 25 mm, fig. 1. The initial structural displacement and velocity are set as 0. The outside of the model is the cooling boundary (liquid nitrogen temperature is −196 °C), which is applied to the convective heat transfer boundary. The liquid nitrogen's heat transfer coefficient, model initial temperature, and thermodynamic parameters are shown in tab. 1. The COMSOL 5.6 software is used for model solving. The heat conduction equation is expressed [12]:

$$\rho c_p \frac{\partial T}{\partial t} - \nabla\left(k\nabla T\right) = Q$$

where ρ is the material density, c_p – the material heat capacity, T – the temperature, t – the time, k – the material thermal conductivity, and Q – the source term.

Table 1. Model parameters

Parameters	Value
Heat transfer coefficients of liquid nitrogen [$Wm^{-2}K^{-1}$]	100, 500, 1000
Initial temperature [°C]	200, 300, 400
Young's modulus [GPa]	10, 20, 30
Expansion coefficient [$\cdot 10^{-6}$ K^{-1}]	8, 10, 12
Poisson's ratio	0.13
Density [kgm^{-3}]	2654
Thermal conductivity [$Wm^{-1}K^{-1}$]	2.6 [13]
Heat capacity [$Jkg^{-1}K^{-1}$]	820 [13]

The thermal-mechanical coupling equations for linear elastic materials are expressed [12]:

$$\rho\frac{\partial^2\mathbf{u}}{\partial t^2}=\nabla\mathbf{S}+\mathbf{F}_\mathrm{V}$$

$$\mathbf{S}=\mathbf{C}\left(E,\mu\right):\boldsymbol{\varepsilon}_\mathrm{el}$$

$$\boldsymbol{\varepsilon}_\mathrm{el}=\frac{1}{2}\left[\left(\nabla\mathbf{u}\right)^T+\left(\nabla\mathbf{u}\right)\right]-\boldsymbol{\varepsilon}_\mathrm{th}$$

$$\boldsymbol{\varepsilon}_\mathrm{th}=\boldsymbol{\alpha}_T\left(T-T_0\right)$$

where $\mathbf{u}$ is the displacement tensor, $\mathbf{S}$ – the stress tensor, $\mathbf{F}_\mathrm{V}$ – the volume force tensor, $\mathbf{C}$ – the fourth order constitutive tensor, E – the Young's modulus, μ – the Poisson's ratio, $\boldsymbol{\varepsilon}_\mathrm{el}$ – the elastic strain tensor, $\boldsymbol{\varepsilon}_\mathrm{th}$ – the thermal strain tensor, $\boldsymbol{\varepsilon}_T$ – the expansion coefficient, and T_0 – the initial temperature.

Effect of heat transfer coefficients

Figure 2 shows the temperatures and maximum principal stresses along A to B after 60 seconds of liquid nitrogen cooling at various heat transfer coefficients. The temperature of the model's exterior in contact with the liquid nitrogen decreases significantly, and the temperature decrease is more pronounced with elevated heat transfer coefficient. The model's exterior exhibits temperature drops from 200-71 °C at 100 W/m^{2}K compared to −147 °C at 1000 W/m^{2}K. This enhancement in cooling rate directly correlates with the heat transfer coefficient, demonstrating convective heat transfer's dominant role in cryogenic shock severity. The higher heat transfer coefficient enhances the cooling efficiency of liquid nitrogen, leading to a more rapid temperature change at the model's exterior under the same cooling time. Also due to the enhanced cooling efficiency, the temperature difference between the interior and exterior of the model becomes larger correspondingly. The model is under tension on the exterior and compression on the interior, and the outer tensile stress increases with the elevated heat transfer coefficient while the inner compressive stress increases accordingly. A higher heat transfer coefficient leads to faster temperature change inside the model during the cooling process, resulting in a larger temperature gradient and more severe cryogenic-induced stress generation in constrained contraction scenarios.

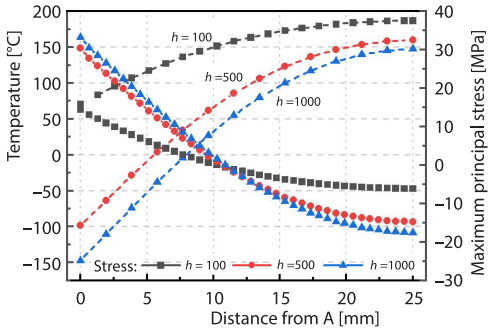

Figure 2. Temperatures and maximum principal stresses along A to B after 60 seconds of liquid nitrogen cooling at various heat transfer coefficients

Figure 3 presents the maximum principal stress distributions during liquid nitrogen cooling at various heat transfer coefficients. During the cooling of the liquid nitrogen in contact with the model's exterior, the maximum value of tensile stress occurs at the exterior surface of the model. As the cooling time increases, the tensile region gradually extends towards the interior of the model. As the model heat transfer coefficient increases, the tensile stress as well as the tensile stress region increases for the same cooling time. This phenomenon arises from Fourier's law-driven temperature gradient intensification within the model, which in turn raises the cryogenic-induced stresses. Experimentally measured tensile strength of granite is approx-

imately 8 MPa [8], the region where the tensile stress exceeds 8 MPa from the exterior to the interior of the model increases accordingly as the heat transfer coefficient increases, indicating an increase in the cryogenic-induced damage depth. The aforementioned results suggest that the cryogenic-induced stresses during the cooling process are sufficient to damage the rock and that the elevated heat transfer coefficient has a significant effect on the stress magnitude and damage area.

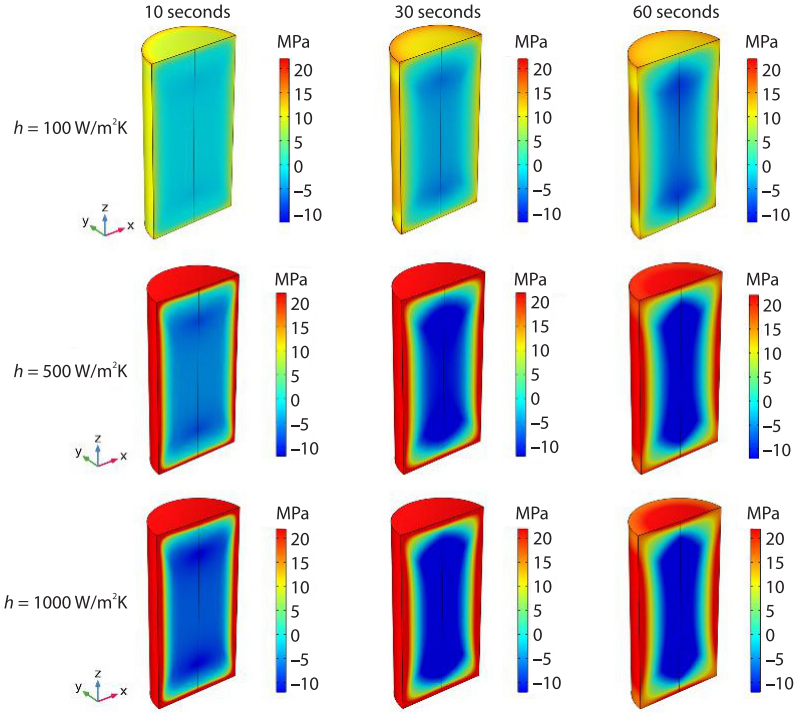

Figure 3. Maximum principal stress distributions during liquid nitrogen cooling at various heat transfer coefficients

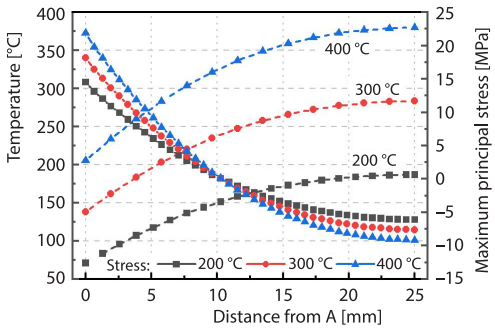

Figure 4. Temperatures and maximum principal stresses along A to B after 60 seconds of liquid nitrogen cooling at various granite temperatures

Effect of model initial temperatures

Figure 4 shows the temperatures and maximum principal stresses along A to B after 60 seconds of liquid nitrogen cooling at various model initial temperatures. As the model's initial temperature increases, the temperature of the exterior decreases more significantly and the temperature difference between the exterior and the interior becomes larger under the same cooling time, which is because the temperature difference between the model and the liquid nitrogen becomes larger as the initial temperature increases and the heat transfer efficiency of the cooling process is increased. The model is under tensile stress on the exterior and compressive

stress on the interior. As the model initial temperature increases, the stresses in both the tensile and compressive zones increase accordingly, which is attributed to the fact that the initial temperature enhances the cooling efficiency, and the magnitude and gradient of temperature change within the model become larger, increasing the constrained deformation and therefore, increasing cryogenic-induced stresses.

Figure 5 presents the maximum principal stress distributions during liquid nitrogen cooling at various granite temperatures. The tensile region on the model's exterior gradually extends into the interior with cooling time. The exterior tensile stresses escalate significantly with increasing initial temperatures, reaching 16.1 MPa at 200 °C compared to 24.3 MPa at 400 °C at 60 seconds, which is attributed to the enhanced temperature difference between the liquid nitrogen and model. The tensile stress region and the tensile damage zone (≥8 MPa) are enlarged with elevated initial temperature. The enhanced temperature difference between liquid nitrogen and the model raises the temperature gradient within the model driven by Fourier's law, inducing greater thermal strain incompatibility. Thus the tensile stress field exhibits both magnitude amplification and spatial extension. These results suggest that liquid nitrogen has the potential to be used for high temperature reservoir stimulation.

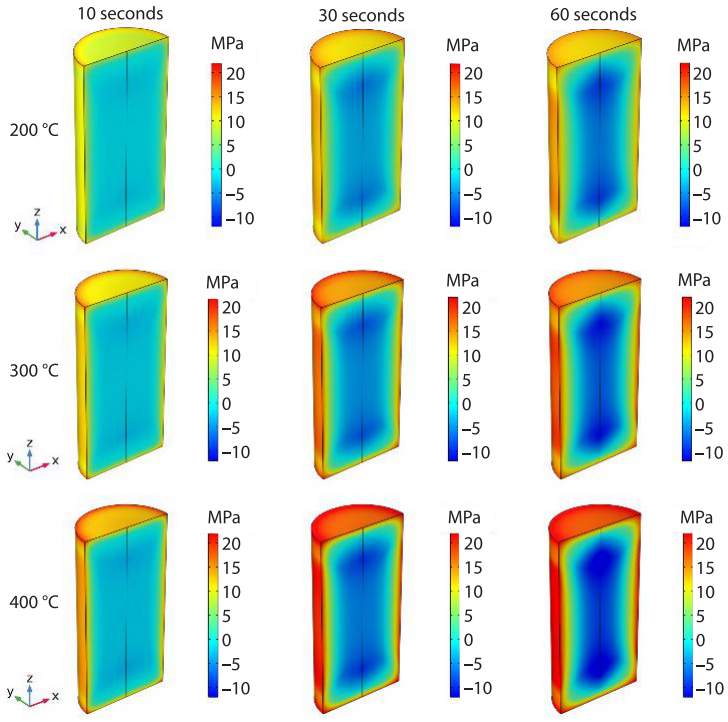

Figure 5. Maximum principal stress distributions during liquid nitrogen cooling at various granite temperatures

Effect of Young's modulus and expansion coefficients

Figure 6 shows the temperatures and maximum principal stresses along A to B after 60 seconds of liquid nitrogen cooling for various Young's modulus and expansion coefficients. The temperature change within the model during cooling is independent of Young's modulus and expansion coefficients. The cryogenic-induced stresses are affected by Young's mod-

ulus and expansion coefficients. For models with different Young's modulus and expansion coefficients, the models are also subjected to external tensile and internal compression due to the same temperature change during the cooling process. Under different Young's modulus, the model deformation is invariable, and the cryogenic-induced stress increases with a higher Young's modulus, fig. 6(a). This phenomenon correlates directly with Hooke's law governing thermal stress formation (*e.g.* if the material is subjected to a uniform temperature change and is completely constrained, the thermal stress is $\sigma = E\alpha\,\Delta T$), where enhanced modulus amplifies stress development under identical thermal contraction constraints. Thus both tensile and compressive stresses are positively correlated with Young's modulus. Under different expansion coefficients, the cryogenic-induced stress increases with a higher expansion coefficient, fig. 6(b), which is attributed to that a high expansion coefficient enhances the thermal strains as well as the thermal strain incompatibility.

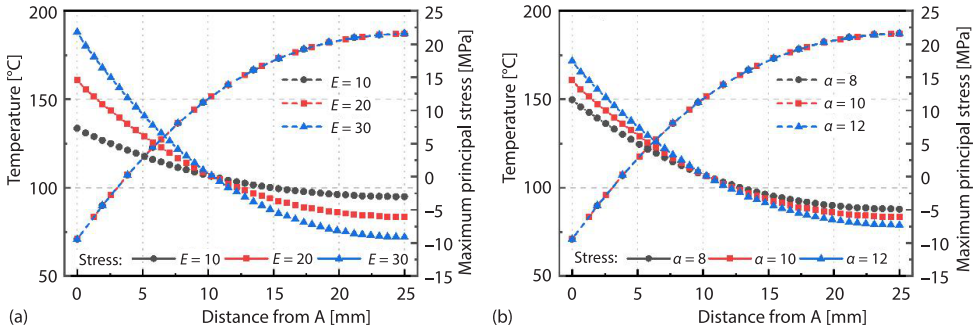

Figure 6. Temperatures and maximum principal stresses along A to B after 60 seconds of liquid nitrogen cooling for various; (a) Young's modulus and (b) expansion coefficients

Figure 7 presents the maximum principal stress distributions during liquid nitrogen cooling for various Young's modulus. The maximum tensile stress manifests at the exterior of the model across all Young's modulus conditions, aligning with fundamental principles of thermal stress generation in constrained contraction scenarios. The tensile region gradually develops towards the model's interior with cooling time. At the same cooling time, the outer tensile stress as well as the stress difference between the interior and exterior are enhanced with Young's modulus. In addition, the tensile damage zone (≥8 MPa) is also enlarged gradually with increasing Young's modulus. Due to the same deformation caused by the same temperature change, higher modulus materials exhibit amplified stress magnitudes due to their enhanced resistance to elastic deformation under equivalent thermal strain conditions, thus increasing the range of the tensile damage zone. Figure 8 presents the maximum principal stress distributions under various expansion coefficients. Under the same temperature difference within the model, the high expansion coefficients enhance the constrained thermal deformation, thus elevating the tensile stress and tensile damage zone.

Conclusion

Numerical simulations of the liquid nitrogen cooling process for standard specimens under different parameters are carried out. It can be concluded that a higher heat transfer coefficient and model initial temperature enhance the heat transfer efficiency of the cooling process, thus resulting in more severe cryogenic-induced stresses. Young's modulus and expansion coefficient are independent of the temperature distribution during the cooling process. Higher

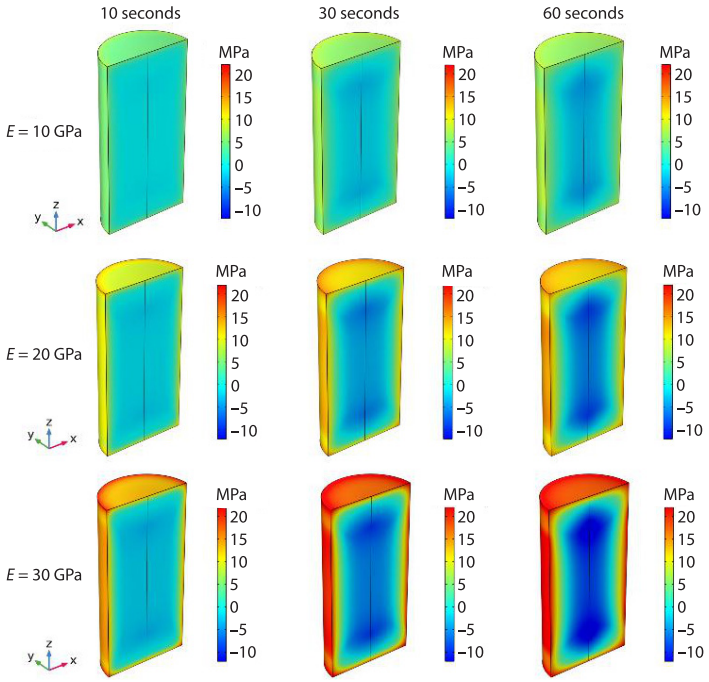

Figure 7. Maximum principal stress distributions during liquid nitrogen cooling for various Young's modulus

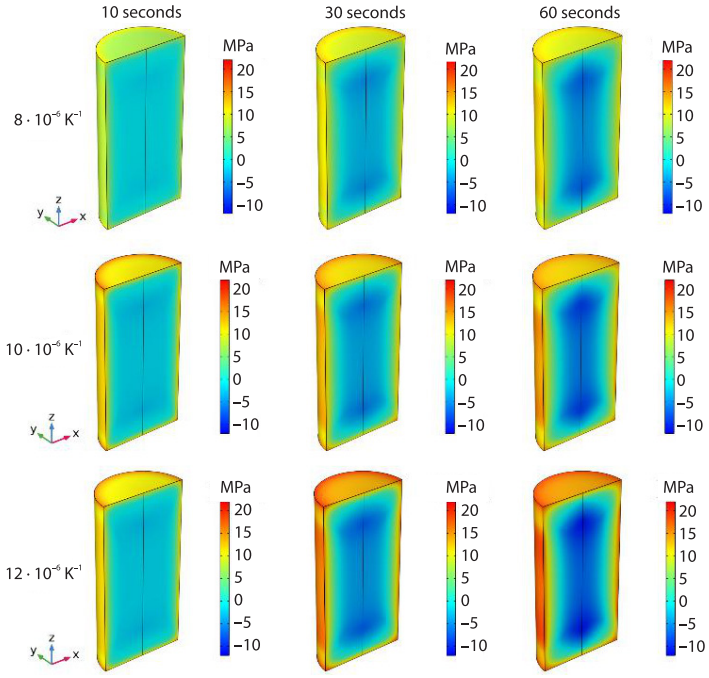

Figure 8. Maximum principal stress distributions during liquid nitrogen cooling for various expansion coefficients

Young's modulus amplifies stress under identical thermal contraction constraints. Higher expansion coefficients enhance the thermal strains and thermal strain incompatibility, thus elevating the cryogenic-induced stresses.

Acknowledgment

This study was supported by the Natural Science Foundation of Shandong Province (No. ZR2024ME108).

Reference

[1] Huang, Z., *et al.*, A Review of Liquid Nitrogen Fracturing Technology, *Fuel*, *266* (2020), 2, ID117040
[2] Yang, R. Y., *et al.,* Non-Contaminating Cryogenic Fluid Access to High-Temperature Resources: Liquid Nitrogen Fracturing in a Lab-Scale Enhanced Geothermal System, *Renewable Energy*, *165* (2021), 3, pp. 125-138
[3] Zhou, C., *et al.,* Integrating Acoustic Emission into a Percolation Model to Evaluate Crack Distribution Characteristics of Heated Granite Subjected to Rapid Cooling, *Results in Physics*, *38* (2022), 3, 105600
[4] Qin, L., *et al.,* Evolution of the Pore Structure in Coal Subjected to Freeze-Thaw Using Liquid Nitrogen to Enhance Coalbed Methane Extraction, *Journal of Petroleum Science and Engineering*, *175* (2019), 3, pp. 129-139
[5] Akhondzadeh, H., *et al.,* Pore-Scale Analysis of Coal Cleat Network Evolution through Liquid Nitrogen Treatment: A Micro-Computed Tomography investigation, *International Journal of Coal Geology*, *219* (2020), 3, ID103370
[6] Hou, P., *et al.,* Effect of Liquid Nitrogen Thermal Shock on Structure Damage and Brittleness Properties of High-Temperature Marble, *Geomechanics and Geophysics for Geo-Energy and Geo-Resources*, *8* (2022), 2, ID69
[7] Wu, X., *et al.,* Damage analysis of high-temperature rocks subjected to LN_2 thermal shock, *Rock Mechanics and Rock Engineering*, *52* (2019), 8, pp. 2585-2603
[8] Zhou, C., *et al.*, Effect of Different Cooling Treatments on the Tensile Properties and Fracture Modes of Granite Heated at Different Temperatures, *Natural Resources Research*, *31* (2022), 2, pp. 817-833
[9] Su, S., *et al*., Changes in Mechanical Properties and Fracture Behaviors of Heated Marble Subjected to Liquid Nitrogen Cooling, *Engineering Fracture Mechanics*, *261* (2022), 2, ID108256
[10] Tang, S., *et al*., Theoretical and Numerical Studies of Cryogenic Fracturing Induced by Thermal Shock for Reservoir Stimulation, *International Journal of Rock Mechanics and Mining Sciences*, *125* (2020), 3, ID104160
[11] Du, M., *et al*., Study on the Surface Crack Propagation Mechanism of Coal and Sandstone Subjected to Cryogenic Cooling with Liquid Nitrogen, *Journal of Natural Gas Science and Engineering*, *81* (2020), 3, ID103436
[12] Hou, P., *et al*., Effect of Liquid Nitrogen Cooling on Mechanical Characteristics and Fracture Morphology of Layer Coal under Brazilian Splitting Test, *International Journal of Rock Mechanics and Mining Sciences*, *151* (2022), 3, ID105026
[13] Wang, F., Konietzky, H., Thermo-Mechanical Properties of Granite at Elevated Temperatures and Numerical Simulation of Thermal Cracking, *Rock Mechanics and Rock Engineering*, *52* (2019), 10, pp. 3737-3755

Paper submitted: July 27, 2024
Paper revised: October 21, 2024
Paper accepted: November 26, 2024